Supplementary Information

Probing Laser-induced Structural Transformation of Lignin into Few-layer Graphene

*Hanwen Zhang [a], Qianwei Li [a], Karl D. Hammond [a], Xiaoqing He [b, c], Jian Lin [b], Caixia Wan [a, *]*

[a] Department of Chemical and Biomedical Engineering, University of Missouri, Columbia 65211, Missouri, USA

[b] Department of Mechanical and Aerospace Engineering, University of Missouri, Columbia 65211, Missouri, USA

[c] Electron Microscopy Core Facilities, University of Missouri, Columbia 65211, Missouri, USA

[*] Corresponding author: Phone: +1 573 884 7882; Fax: +1 573 884 5650; E-mail: wanca@missouri.edu

Number of tables: 2

Number of figures: 11

Table S1. Assignments of main ^{13}C-^{1}H cross-signals of lignin in 2D HSQC spectra.

Lignin subunits	Chemical shift (δC/δH (ppm))
C_α–H_α in β–O–4′ (A)	71.1/4.8
C_α–H_α in β–5′ (B)	86.4/5.5
C_α–H_α in β–β′ (C)	84.7/4.6
C_β–H_β in Secoisolariciresinols (D)	42.3/1.9
C_α–H_α and C_β–H_β in Stilbenes (E)	128.2/7.1
C_2–H_2 in G units	110.3/6.9
C_5–H_5 in G units	115.0/6.7
C_6–H_6 in G units	118.3/6.8

Table S2. Specification of two starting systems in MD simulation.

Lignin model	Molecular formula	Molecular Weight (g/mol)	Number of molecules	Total atoms	Density (g/cm^3)	Total Carbon atoms
G2	$C_{17}H_{20}O_6$	320	29	1247	1.18	493
G6	$C_{57}H_{68}O_{22}$	1104	8	1176	1.16	456

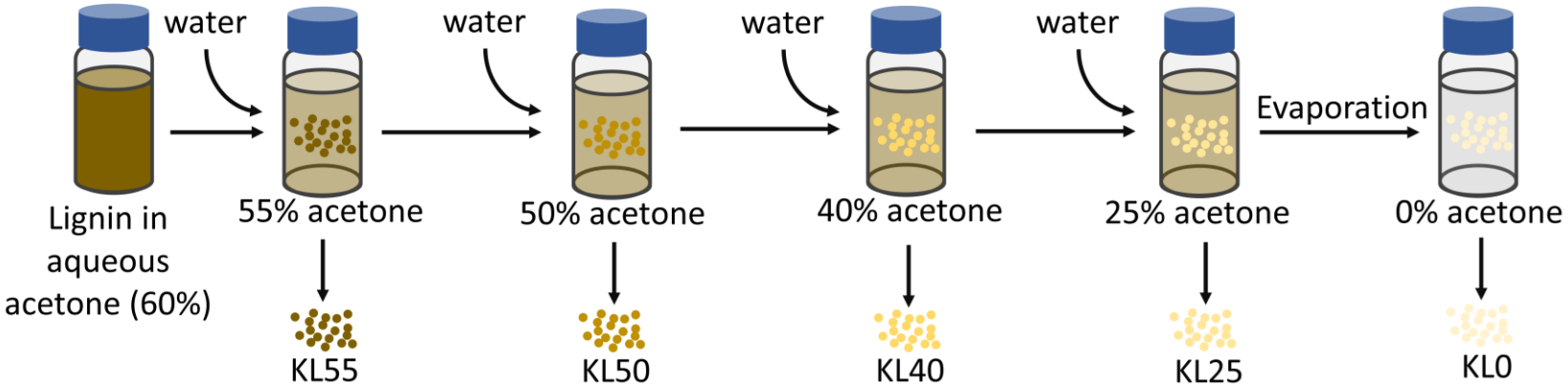

Figure S1. Schematic diagram of the kraft lignin fractionation/refining process. Acetone content in acetone-water mixture is referred to the percentages of pure acetone mixed with water by volume.

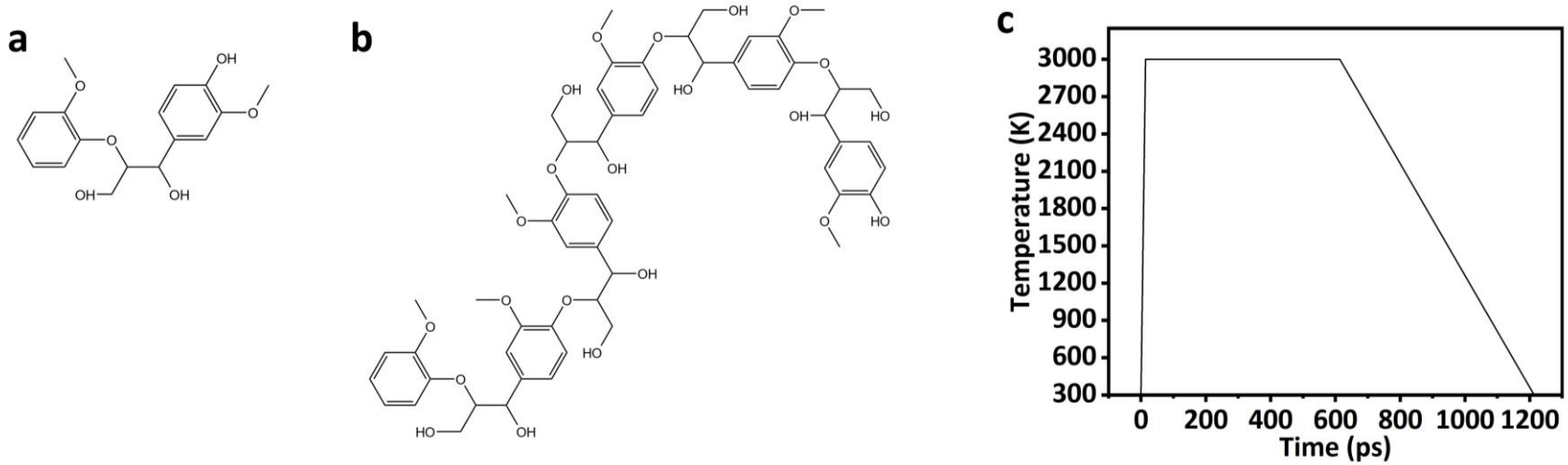

Figure S2. 2D model structure of (a) G2 and (b) G6. (c) The temperature profile of the simulation system. The system was first ramped from 300 K to 3000 K at 200K/ps and kept at 3000 K for 600 ps. Eventually, the system was cooled down from 3000 K to 300K for another 600 ps.

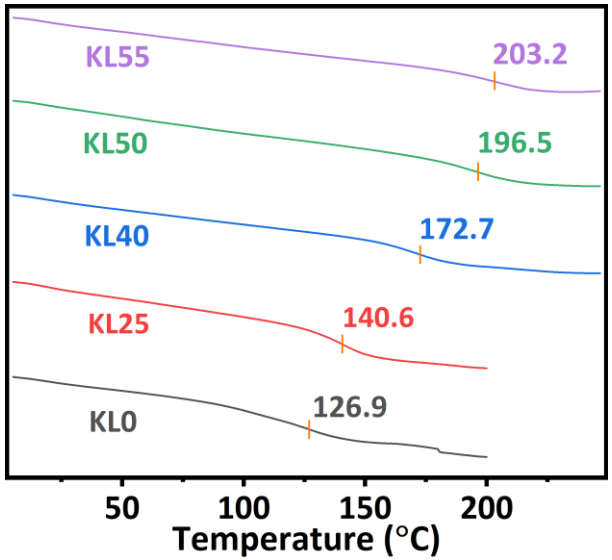

Figure S3. Differential scanning calorimetry (DSC) curves of the lignin fractions.

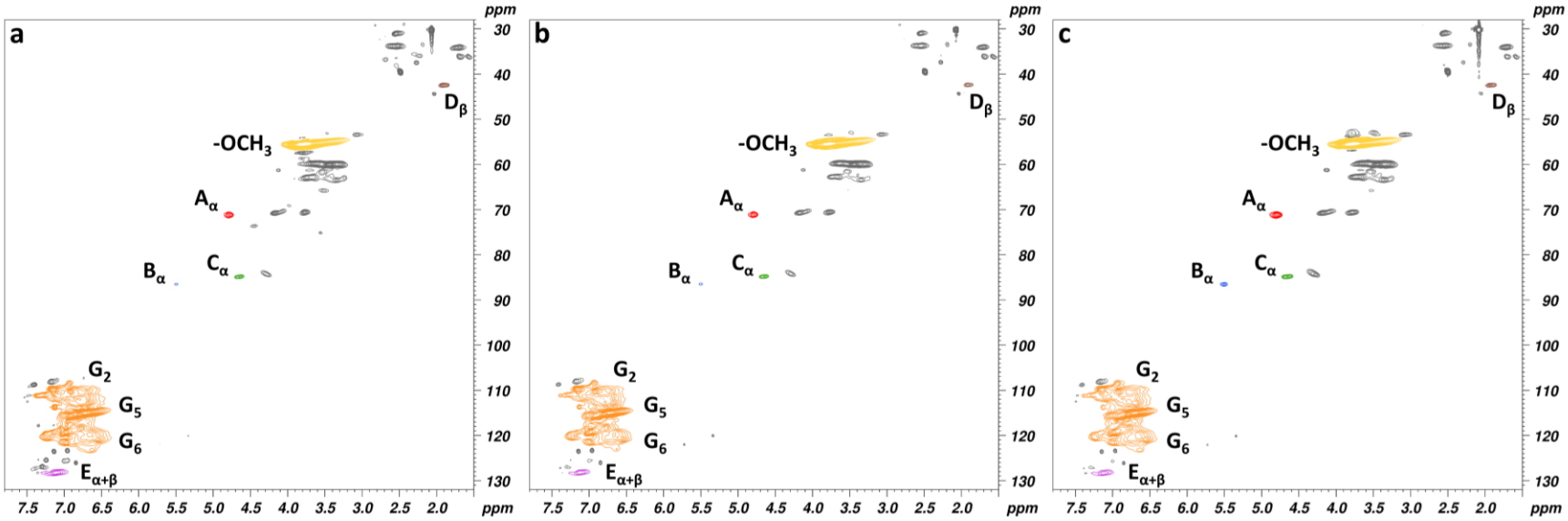

Figure S4. 2D HSQC NMR spectra of the lignin fractions: (a) KL25, (b) KL40, (c) KL50.

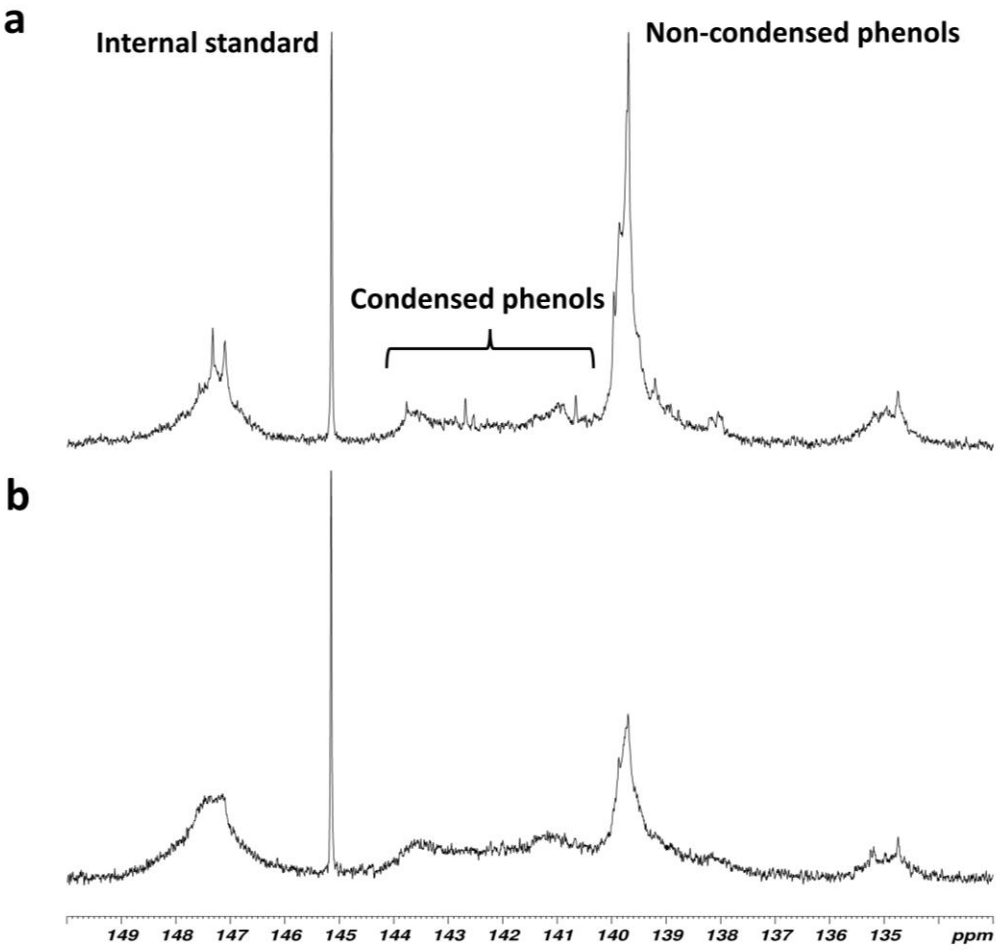

Figure S5. ^{31}P NMR spectra of (a) KL0 and (b) KL55.

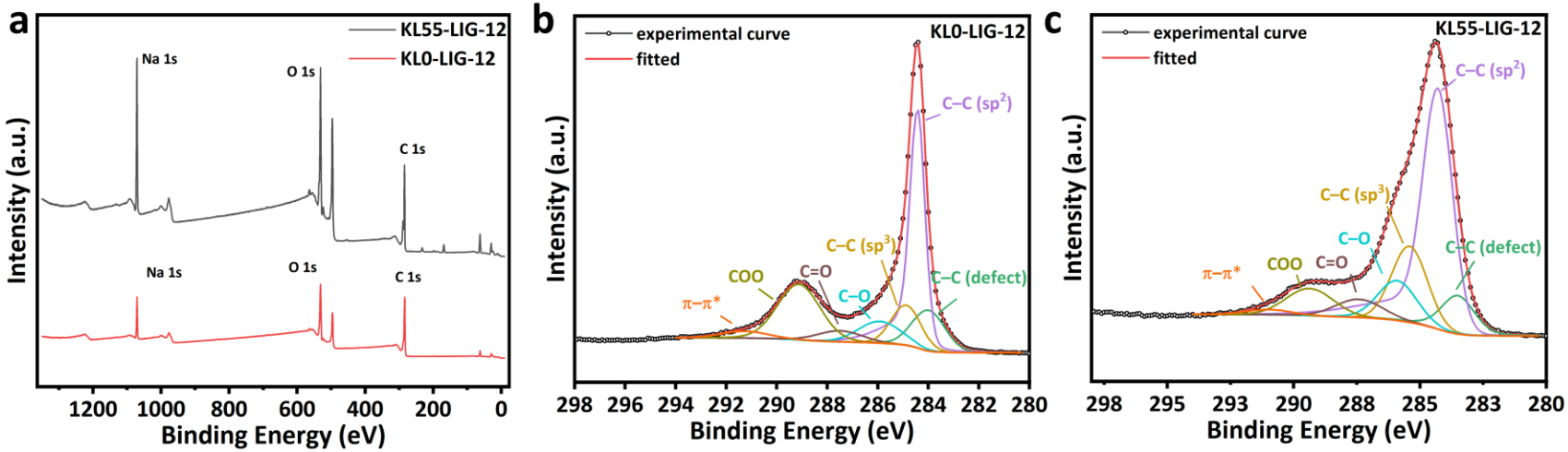

Figure S6. (a) X-ray photoelectron spectroscopy (XPS) survey spectra of KL55-LIG-12 and KL0-LIG-12. High resolution C 1s XPS spectrum of (b) KL0-LIG-12, and (c) KL55-LIG-12.

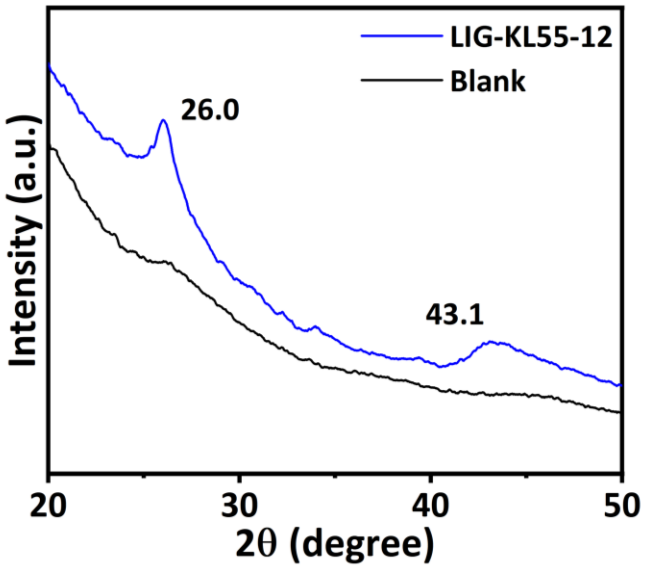

Figure S7. XRD of LIG-KL55-12.

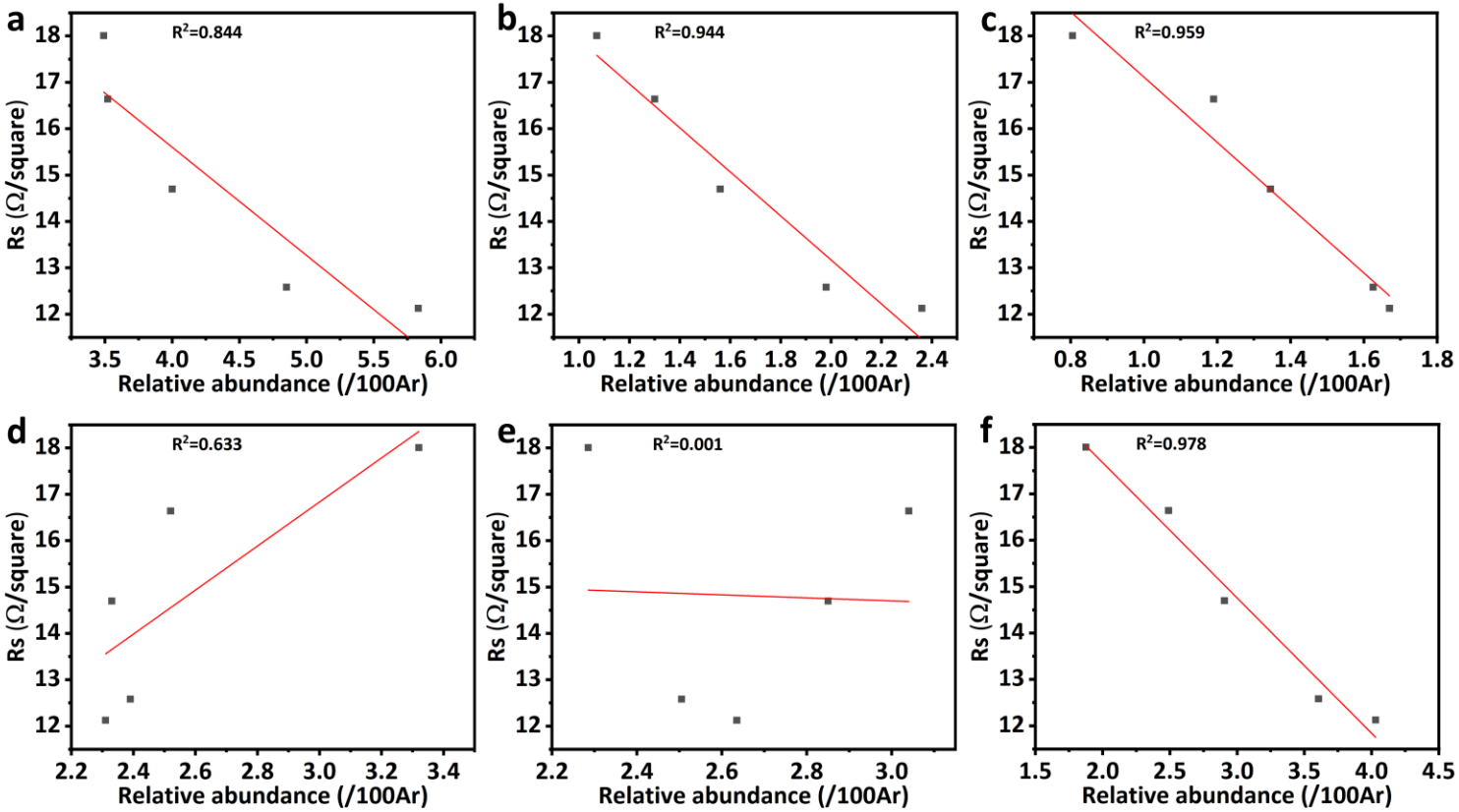

Figure S8. The linear regression analysis of the relative abundance of lignin interlinkages contents and Rs of LIG at 14% power. (a) A vs Rs; (b) B vs Rs; (c) C vs Rs; (d) D vs Rs; (e) E vs Rs; (f) B&C vs Rs.

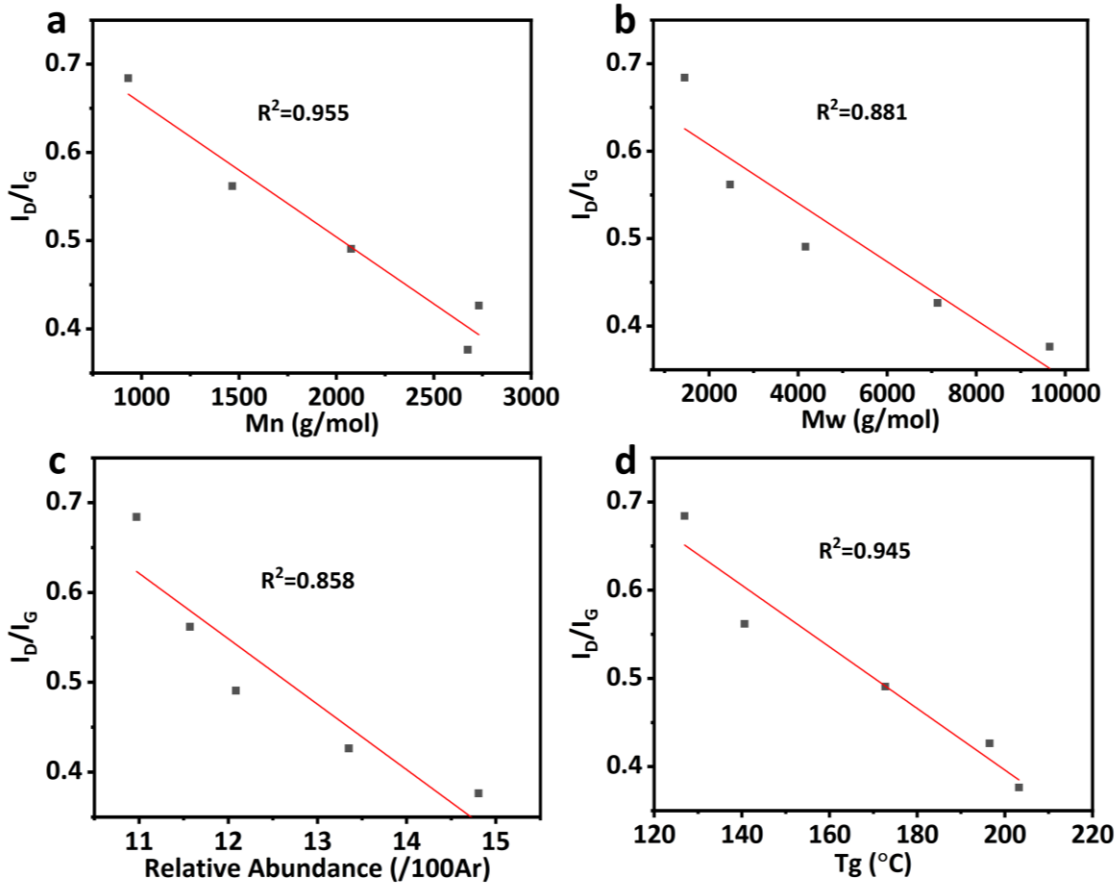

Figure S9. The linear regression analysis of the relative abundance of lignin's main characteristics and the corresponding Raman peak ratios of LIG formed at 12% power. (a) M_n; (b) M_w; (c) Relative abundance; (d) T_g.

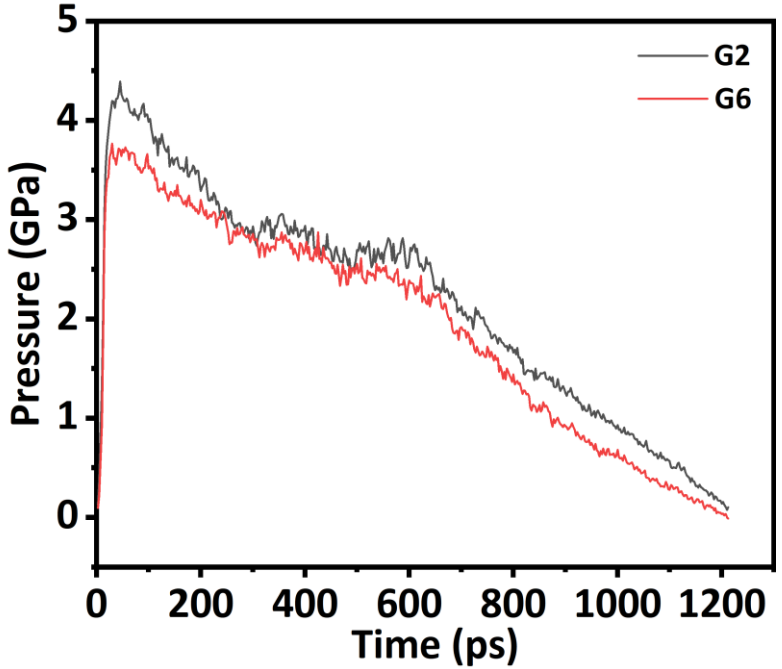

Figure S10. The pressure evolution of different simulation systems

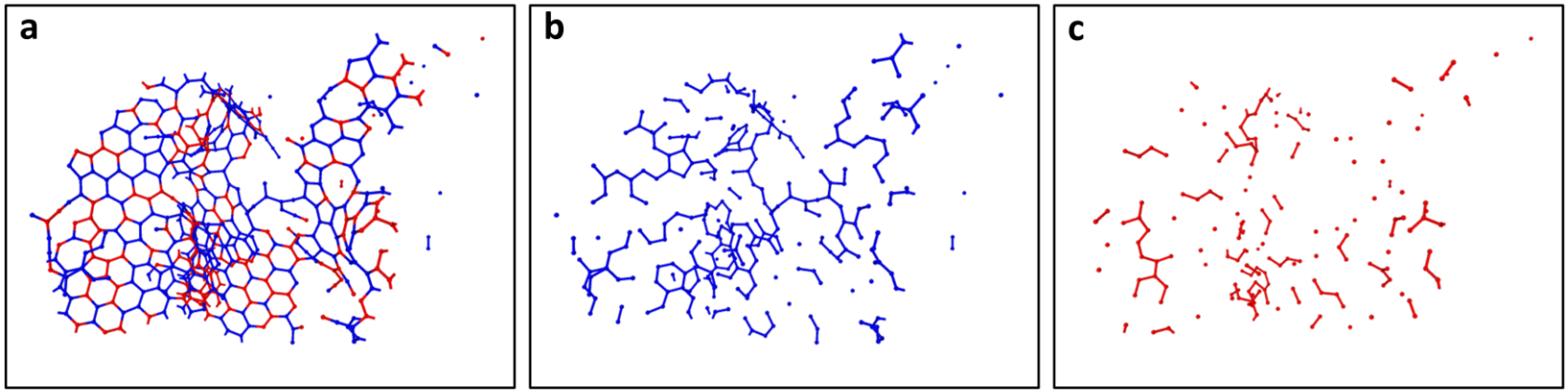

Figure S11. Snapshots of final simulation system from G6 (Carbon atoms only). (a) all carbon atoms; (b) aromatic carbon atoms only; (c) aliphatic carbon atoms only. The blue atoms are the aromatic carbon atoms. The red atoms are the aliphatic carbon atom in the initial system.